SOI Mach-Zehnder Interferometer Design, Fabrication, and Analysis

Ameer Ibrahim Osman, Ameer.IbrahimOsman@mail.mcgill.ca

Department of Electrical and Computer Engineering, McGill University, Montreal, H3A 0G4, Canada

I. Introduction

Silicon photonics has recently made significant progress in optical communications. The combination of photonics and electronics to improve and optimize the architecture of communications systems is crucial to many modern challenges such as the hindering of Moore's Law. An important device in optical communications is the Mach-Zehnder Interferometer (MZI). It is used in switching, modulation, and multiplexing [2] of optical signals.

This paper aims to design the MZI utilizing a Silicon-On-Insulator (SOI) wafer. The design incorporates strip waveguides, Y branch splitters, & Y branch combiners.

We firstly introduce the components used and the relevant theory in section 2. This includes the phenomenon of interference, which is the heart of the MZI mechanism. Section 3 presents the simulation setup and its theoretical results. Section 4 describes the fabrication process, and section 5 presents the experimental data. Section 6 analyzes the experimental data, & section 7 concludes the paper.

II. Theory

Firstly, a brief overview of the concepts & components used in the MZI. The term SOI refers to a silicon layer buried in a silicon dioxide insulator. The difference in refractive index between these two materials allows for a wave to be guided in the silicon layer. The SOI is shown in the following figure:

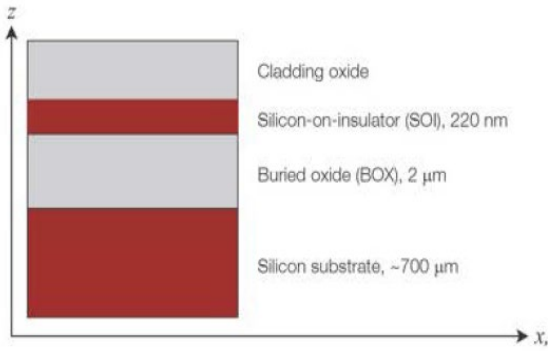

Figure 1: Cross sectional view of the Silicon on insulator wafer.

The Y-branch splitter is a device of one input and two outputs. At the input is the quasi-TE wave of electric field E_i and corresponding intensity I_i. As the name suggest, the wave is split into two waves of electric fields $E_1 = E_2 = \frac{E_i}{\sqrt{2}}$ and intensities $I_1 = I_2 = \frac{I_i}{2}$. The split waves then propagate through two strip waveguides of potentially differing lengths L_1 & L_2. After which, the waves are recombined via the Y-branch combiner. The combiner outputs the combination of the two input waves as characterized by $E_o = \frac{E_1 + E_2}{\sqrt{2}}$. The figure below showcases the combination of these components to form the MZI.

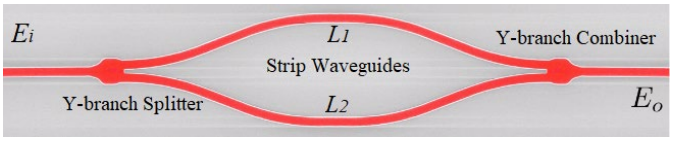

Figure 2: Balanced MZI composed of Y branch splitter, Strip waveguides, and a Y branch combiner.

Approximating the MZI's input wave as a plane wave allows us to derive it's transfer function. A plane wave's electric field can be described with the following equation:

$$E = E_A\, e^{i(\omega t - \beta z)} \quad (1)$$

Where E_A is the electric field's amplitude, ω is the fields angular frequency, & β is the field's propagation constant defined as $\beta = \frac{2\pi n}{\lambda}$, where n is the refractive index of the medium and λ is the wavelength of the field. Denoting the electric field output of the Y branch splitter in the MZI as E_{o1} & E_{o2}, they are described by plane waves of differing parameters (lossless case), that is:

$$E_{o1} = E_{A1}\, e^{-i\beta_1 L_1} = \frac{E_i}{\sqrt{2}} e^{-i\beta_1 L_1} \quad (2)$$

$$E_{o2} = E_{A2}\, e^{-i\beta_2 L_2} = \frac{E_i}{\sqrt{2}} e^{-i\beta_2 L_2} \quad (3)$$

Thus, the output of the Y branch splitter is:

$$E_o = \frac{E_{o1} + E_{o2}}{\sqrt{2}} = \frac{E_i}{2}\left(e^{-i\beta_1 L_1} + e^{-i\beta_2 L_2}\right) \quad (4)$$

With output Intensity

$$I_o = \frac{I_i}{4}\left|e^{-i\beta_1 L_1} + e^{-i\beta_2 L_2}\right|^2$$

$$I_o = \frac{I_i}{2}[1 + \cos(\beta_1 L_1 - \beta_2 L_2)] \quad (5)$$

It is to note that when $\beta_1 = \beta_2$ & $L_1 = L_2$ the MZI configuration is said to be balanced. When the lengths of the two waveguides aren't equal, the MZI's transfer function can be written as:

$$H_{MZI}(\lambda) = \frac{I_o}{I_i} = \frac{1}{2}[1 + \cos(\beta \Delta L)] \quad (6)$$

The free spectral range (FSR) describes the spectral separation of the wavelength modes. The FSR can be described by:

$$FSR = \Delta\lambda = \frac{\lambda^2}{\Delta L n_g} \quad (7)$$

Where n_g is the group index of the wave, which is described by:

$$n_g(\lambda) = n_{eff}(\lambda) - \lambda \frac{dn_{eff}(\lambda)}{d\lambda} \quad (8)$$

Where $n_{eff}(\lambda)$ is the effective refractive index.

III. Modelling and Simulation

A. Waveguide Modelling

The strip waveguide we employ in our design is of height 200nm and width of 500nm. The height is industry standards and is a constraint of the fabrication process. The width of 500nm is selected as it allows near single mode operation. Figure 3 displays the Electric field modal profile and table 1 summarizes the effective indices for the first 4 modes, at an operating wavelength of 1550nm.

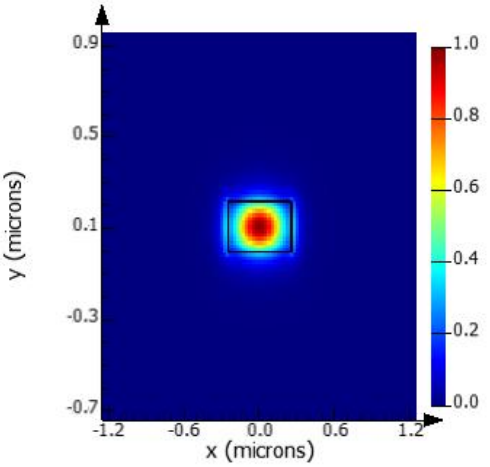

Figure 3: First Quasi-TE modal profile showcasing the normalized Electric field intensity in an x-y cross section at 1550nm of wavelength.

Mode	n_{eff}
TE1	2.4473
TM1	1.7689
TE2	1.4965
TM2	1.3467

Table 1: Quasi-Transverse modes and their corresponding effective indices at an operating wavelength of 1550nm.

The guided modes are approximately the first 3 entries of table 1, as their effective indices are higher

than that of the surrounding silicon dioxide (1.444 at operation of 1550nm of wavelength). It is important to note that the imaginary part of the effective indices of the modes in table 1 are neglected due to their small contribution in loss. Figures 4 & 5 display the variation in group index and effective index, respectively, with varying operational wavelengths of 1550nm to 1600nm.

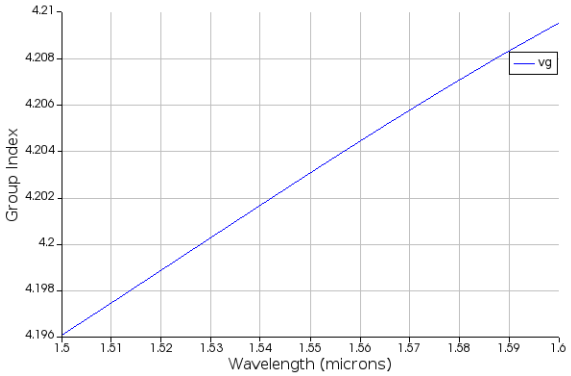

Figure 4: Variation in Group Index with respect to wavelength for the TE1 mode.

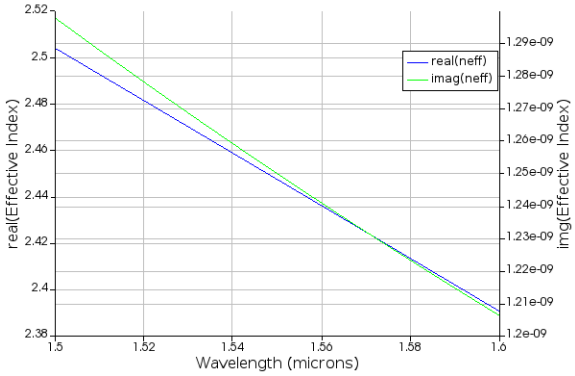

Figure 5: Variation in effective index with respect to wavelength for the TE1 mode.

The effective index plot can be described by a taylor series expansion of three coefficients:

$$n_{eff}(\lambda[\mu m]) = 2.4473 - 1.1326(\lambda - 1.55) - 0.0439(\lambda - 1.55)^2 \quad (9)$$

The results in this section are all obtained from the Lumerical MODE software.

B. MZI Simulation & Analysis

The simulation performed in this section is done on Lumerical INTERCONNECT. The figure below show's the MZI simulation setup.

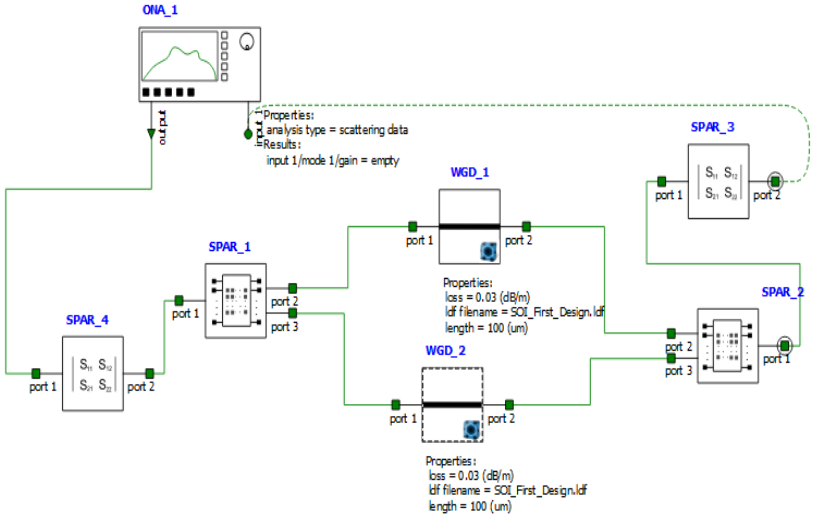

Figure 6: MZI simulation setup showcasing different components & the Optical Network Analyzer (ONA).

The grating couplers are introduced to more accurately simulate the MZI. They provide light coupling as a means of input and output to the MZI. The grating coupler is characterized to display its insertion loss as shown in figure 7. The best-case insertion loss for two grating couplers is found to be 5.087 dB, at 1550nm of operational wavelength.

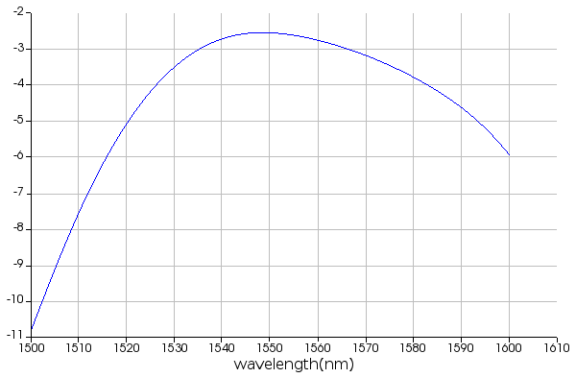

Figure 7: Transfer function showcasing Insertion loss as a function of wavelength for a single grating coupler.

The Y branch splitter & combiner are modeled as S-Matrices. The Y branch splitter & combiner are characterized to display their insertion loss as shown in figure 8.

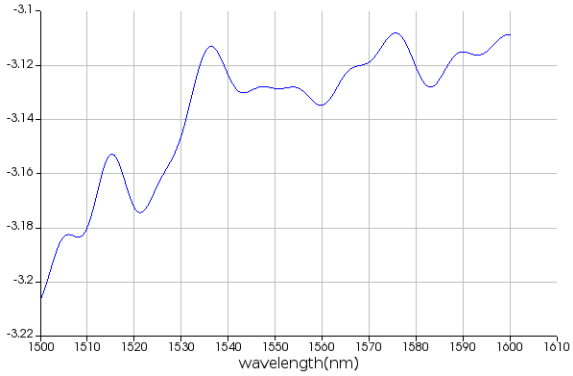

Figure 8: Transfer function showcasing Insertion loss as a function of wavelength for the Y branch splitter & combiner.

The following figures display the gain or the transfer function's for MZI's of various lengths. It is important to note that for a 0 µm length mismatch, there may still be a mismatch due to fabrication issues.

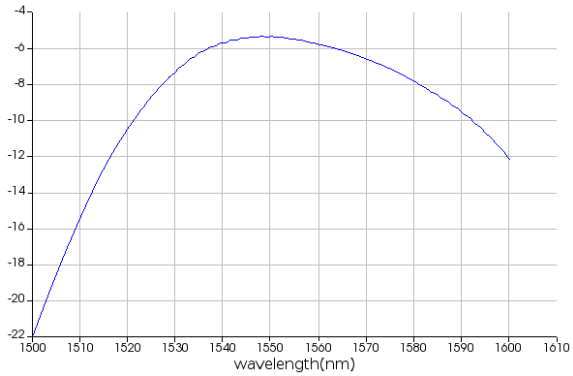

Figure 9: Balanced MZI transfer function (No length mismatch). Note: The y-axis unit's is in dB.

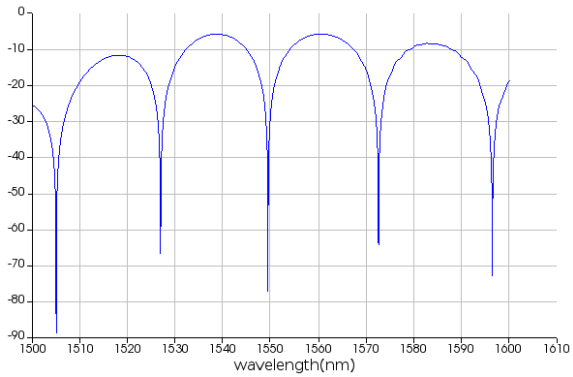

Figure 10: MZI transfer function for a length mismatch of 25µm. Note: The y-axis unit's is in dB.

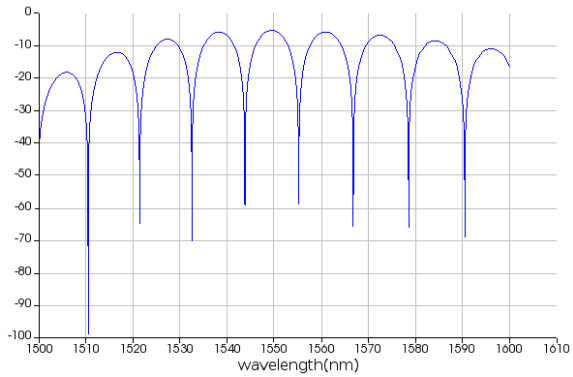

Figure 11: MZI transfer function for a length mismatch of 50µm. Note: The y-axis unit's is in dB.

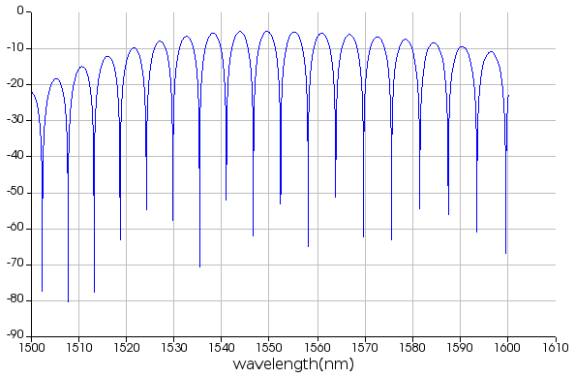

Figure 12: MZI transfer function for a length mismatch of 100µm. Note: The y-axis unit's is in dB.

Figures 9 – 12 show that as the mismatch increases, the number of oscillations in the transfer function of the MZI increase as well.

The transmission spectrum of a length mismatch of 100µm is shown in figure 13.

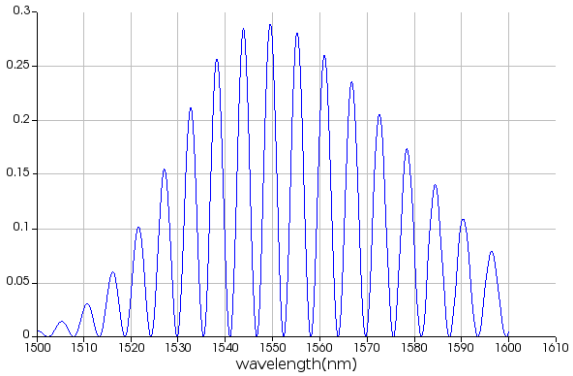

Figure 13: Transmission spectrum of an unbalanced MZI with length mismatch of 100µm on the squared absolute scale. Note: The y-axis unit's is in dB.

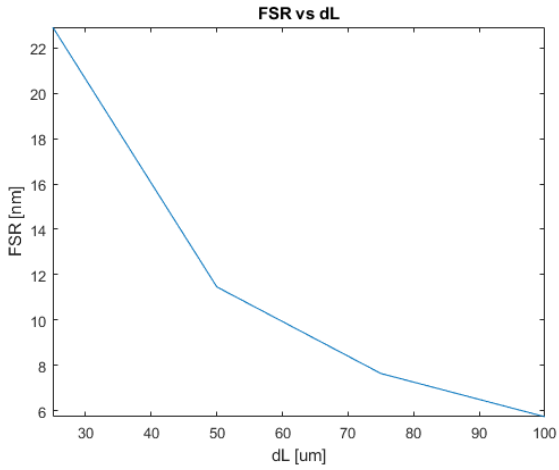

Figure 14: Theoretical variation in FSR plotted against MZI path length mismatch.

IV. Fabrication

A. Layout

The design was developed using the KLayout software [5]. The design includes 8 MZI configurations, of path length mismatch(es) of 0, 25, 50, & 100 µm. Furthermore, one MZI is used to test the 50-50% broadband splitter. The MZI's are on a 605 x 410 µm grid, as can be seen in figure 14.

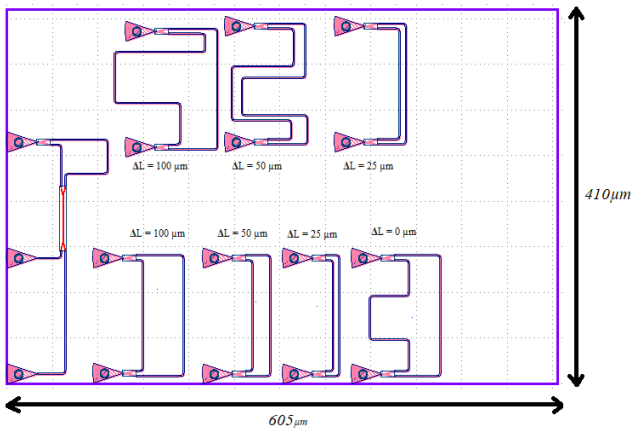

Figure 15: The 8 MZI's depicted in the KLayout software.

There are a few restrictions involved in creating this layout. Firstly, the input & output grating couplers' pitch is fixed to 127 µm. Second, the TE grating couplers are oriented facing the left side, for ease in testing.

B. Fabrication Process

The layout GDS file was sent to the University of Washington's Nanofabrication Facility for fabrication. The facility utilizes a 100keV Electron Beam Lithography (EBL) process for fabrication. This process starts with a SOI wafer. The wafer is spin coated at 4000rpm with hydrogen silsesquioxane resist (HSQ) layer and baked at 80° C for 4 minutes. Then the wafer is exposed to the electron beam, at an exposure dose of 2800 μC/cm^2. The resist is then developed by immersion in 25% tetramethylammonium hydroxide for 4 minutes. Next, it is rinsed with deionized water for 60 seconds, isopropanol for 10 seconds and then it is blown dry with nitrogen. Inductively coupled Plasma etching is then used to remove silicon from unexposed areas, by utilizing chlorine gas. Then, 2-3μm of Oxide is deposited on the wafer, by utilizing the process of plasma enhanced chemical vapor deposition (PECVD), to protect the wafer from surface changed & mechanical damage. Finally, the wafer is diced.

C. Manufacturing challenges

The fabrication process has intrinsic variability that may result in an error in the thickness and width of the waveguide. Thus, a corner analysis is performed to take these errors into account in calculation of the MZI's parameters, specifically, the group index, effective index, and FSR. According to the University of Washington's Nanofabrication facility, there is a variation of ±20nm in waveguide width. Furthermore, there is a thickness variation of ±3.9nm from 219.2nm. The corner analysis for fundamental quasi-TE mode for the various waveguide dimensions is shown in figure 15.

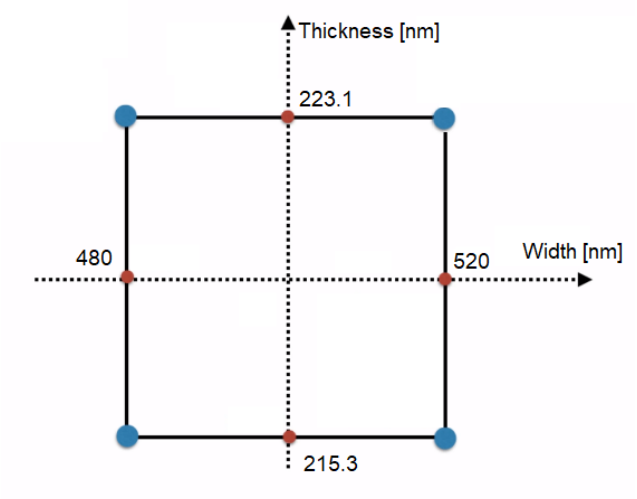

Figure 16: Corner Analysis of various waveguide dimensions.

The results of the corner analysis are summarized in the table(s) below.

Tables 2 & 3: Corner analysis results summarized. The analysis is done at a wavelength of 1550nm. Furthermore, the FSR is calculated for MZI 2 (ΔL = 100 μm), MZI 3 (ΔL = 50 μm), MZI 4(ΔL = 25 μm), & MZI 5(ΔL = 0 μm). Note that in calculation of the FSR for MZI 5, ΔL is approximated to 1 μm.

Corner #	**Dimensions [nm]**	**Group Index**	**Effective Index**
Nominal	500 x 219.2	4.1926	2.4403
1	480 x 223.1	4.2318	2.4198
2	520 x 223.1	4.1649	2.4834
3	520 x 215.3	4.1587	2.4566
4	480 x 215.3	4.2248	2.3924

Corner #	**FSR MZI 2 [nm]**	**FSR MZI 3 [nm]**	**FSR MZI 4 [nm]**	**FSR MZI 5 [nm]**
Nominal	5.7302	11.4601	22.9208	573.0200
1	5.6771	11.3543	22.7087	567.7186
2	5.7684	11.5368	23.0737	576.8440
3	5.7776	11.5540	23.1086	577.7016
4	5.6866	11.3732	22.7464	568.6607

V. Experimental Data

The figure(s) below showcase the baseline fit for MZI's 2, 3, & 4.

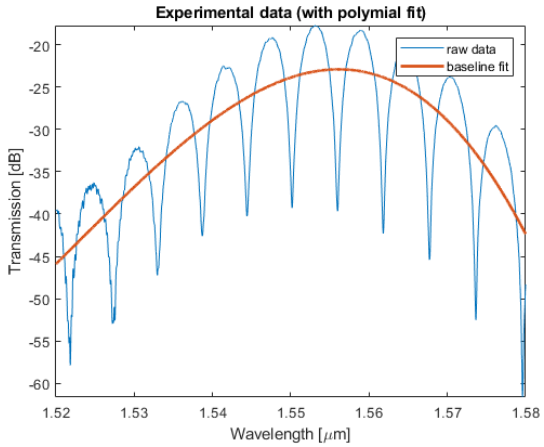

Figure 17: Raw data and baseline correction for TE MZI 2 (100 μm path mismatch).

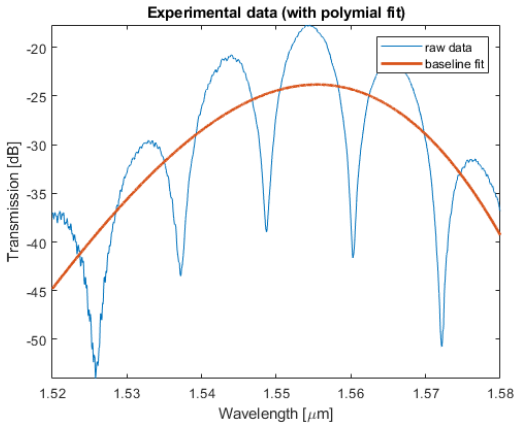

Figure 18: Raw data and baseline correction for TE MZI 3 (50 μm path mismatch).

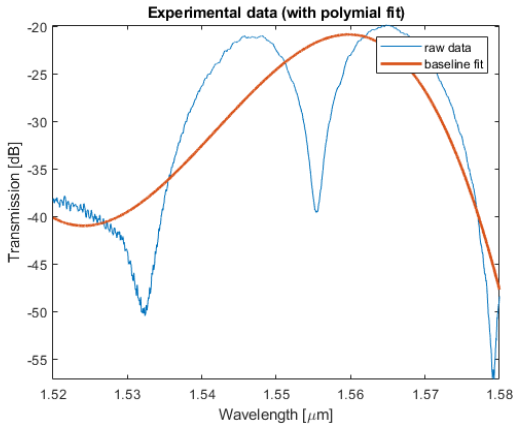

Figure 189: Raw data and baseline correction for TE MZI 4 (25 μm path mismatch).

The baseline fit is calculated using a 3rd order polynomial fit. The baseline fit approximates the transfer function of the MZI. It appears to accurately approximate this transfer function, and hence there isn't a need to use de-embedding devices for correction.

VI. Analysis

The analysis was done for 25°C at a wavelength of 1550nm. The figure below showcases the baseline corrected transfer functions for these MZIs.

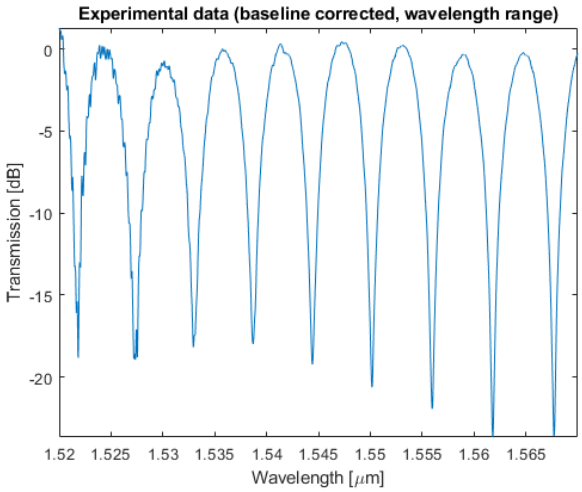

Figure 19: Baseline corrected MZI transfer function for MZI 2 (100 μm path mismatch).

The MZI's transfer function is to be matched to the following equation:

$$F = 10\log\left[\frac{1}{4}\left|1 + e^{i\frac{2\pi n_{eff}}{\lambda}\Delta L - \alpha\frac{\Delta L}{2}}\right|\right]^2 + b$$

Where α is the waveguide loss & b is the excess loss. The following figure depicts the fitting of the baseline corrected transfer function of MZI 2.

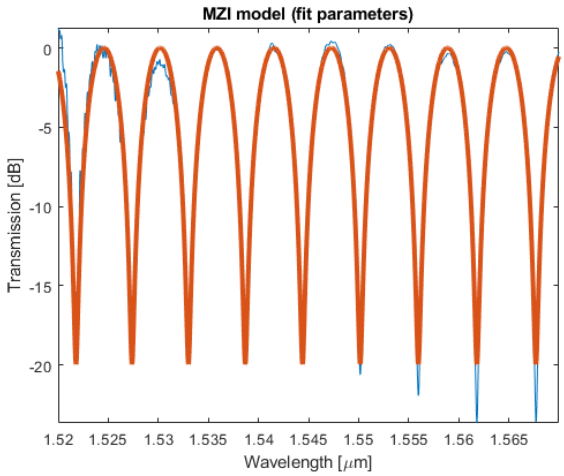

Figure 20: Data fit for baseline corrected transfer function of MZI 2 (TE).

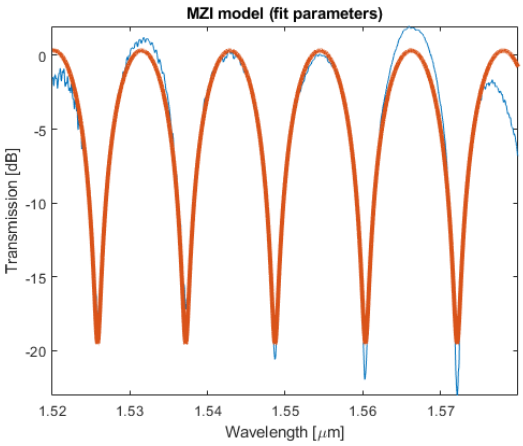

Figure 21: Data fir for baseline corrected transfer function of MZI 3 (TE).

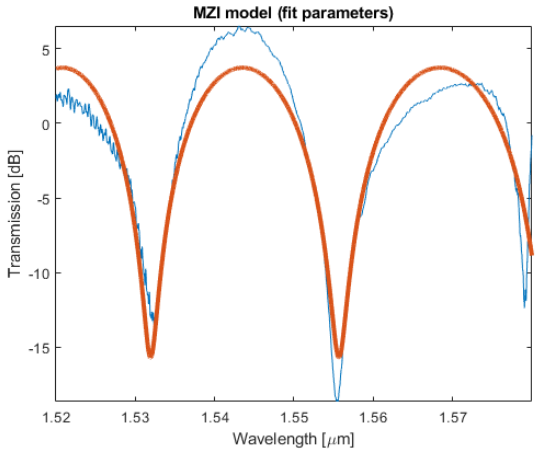

Figure 22: Data fit for baseline corrected transfer function of MZI 4 (TE).

It is to note that the baseline correction of MZI 5 did not work, as the path length mismatch is approximately 0 µm.

It is found that for MZI 2, $n_{eff} = [n_1, n_2, n_3] = [2.3861, -1.1457, 0.016]$, α = 0.0036 dB , & b = 0.9892 dB. The group index is found to be 4.1555 at 1550 nm wavelength which is in range of our corner analysis calculations. The error for the group index is found to be 0.89%. Furthermore, the plots below showcase the effective index, experimental group index, & the FSR for MZI 2, 3, & 4.

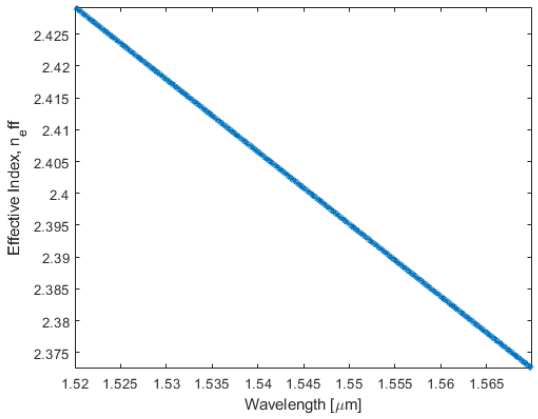

Figure 23: Experimental effective index for MZI 2.

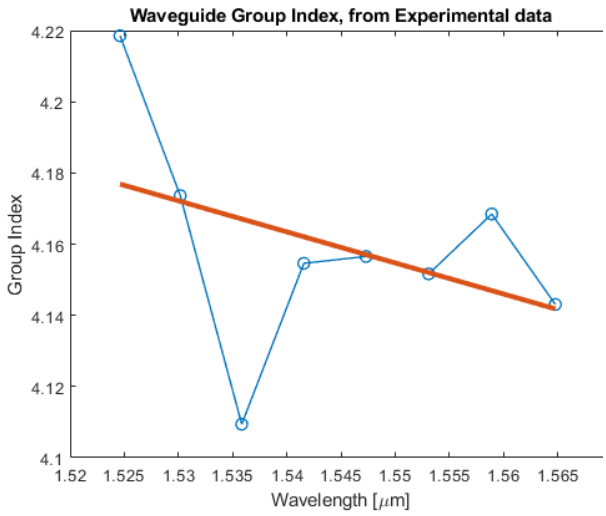

Figure 24: Experimental group index for MZI 2.

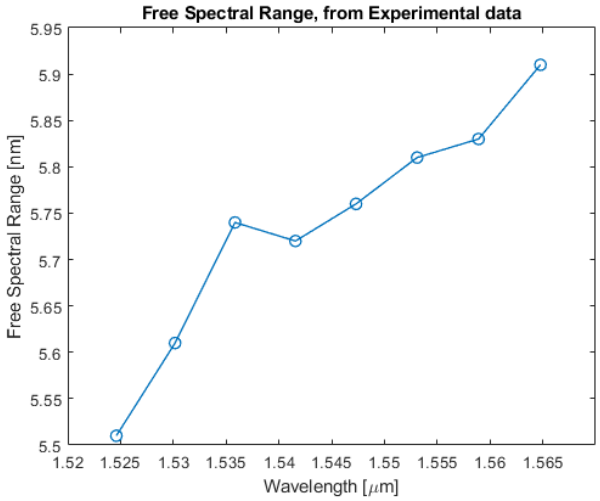

Figure 25: Experimental FSR for MZI 2.

The experimental FSR for MZI 2 is 5.76nm which is in the range of the corner analysis for a wavelength of 1550nm, with an error of 0.517%.

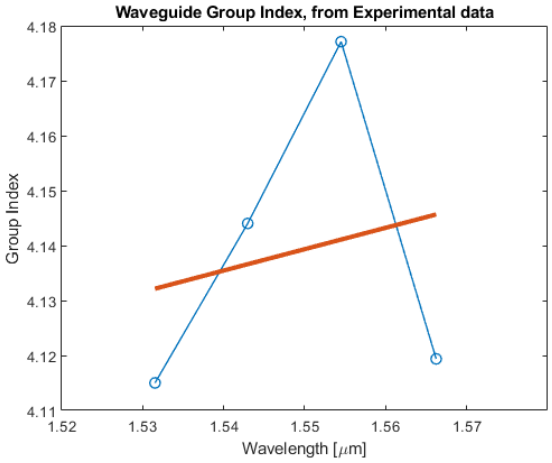

Figure 26: Experimental group index for MZI 3.

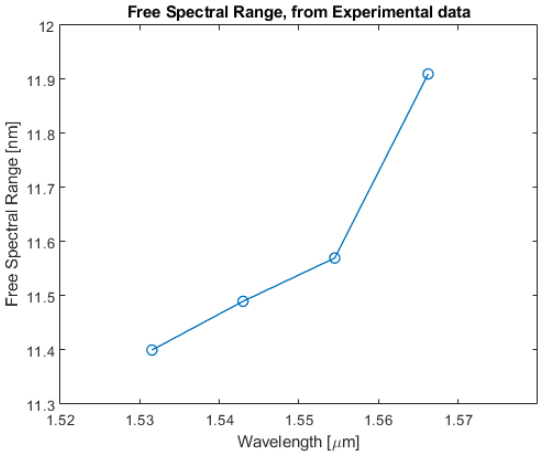

Figure 27: Experimental FSR for MZI 3.

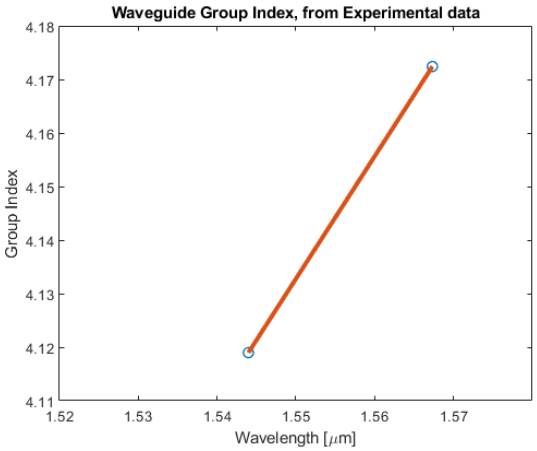

Figure 28: Experimental group index for MZI 4.

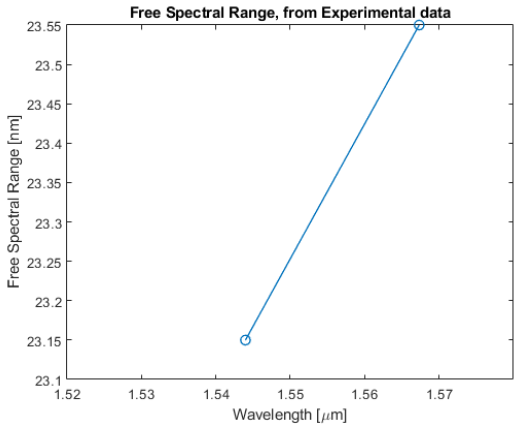

Figure 29: Experimental FSR for MZI 4.

Table 3: Summary of MZI device(s) experimental FSR, Group index, Dispersion, and error(s). Note that as MZI 5's path length is approximately 0, the data is too noisy for analysis.

	FSR [nm]	**Group Index**	**Dispersion [ps/nm/km]**	**FSR error [%]**	**Group Index Error [%]**
MZI 2	5.760	4.155	-164.406	0.517	0.904
MZI 3	11.543	4.135	2409.810	0.718	1.392
MZI 4	23.253	4.1289	-33523.797	1.428	1.542

Table 4: Summary of MZI device(S) experimental n1, n2, n3, waveguide loss, and excess loss.

	n1	**n2**	**n3**	**α [dB]**	**b [dB]**
MZI 2	2.386	-1.145	0.016	0.0036	0.989
MZI 3	2.382	-1.140	-0.235	0.0081	1.167
MZI 4	2.358	-1.155	3.279	0.0171	4.612

VII. Conclusion

This report covers the design of an MZI, utilizing SOI technology. The devices used to create the MZI were introduced, along with a derivation of relevant equations such as the MZI transfer function. Lumerical mode was used to design the waveguides of dimensions 220nm by 500nm. Lumerical interconnect was used to characterize the MZI, & KLayout to create the GDS layout files for fabrication. A corner analysis was performed to take into account the manufacturing variability of the MZI.

The group index and FSR were the main parameters used to characterize & compare the MZIs, and the results for MZI's 2-4 were provided. In comparison of theoretical and experimental values, it is found that a maximum error of 1.54% for both the FSR and group index.

VIII. References

[1] Pérez, D., Gasulla, I., Crudgington, L. *et al.* Multipurpose silicon hotonics signal processor core. *Nat Commun* 8**,** 636 2017. https://doi.org/10.1038/s41467-017-00714-1

[2] Y. Hibino *et al*., "Wavelength division multiplexer with photoinduced Bragg gratings fabricated in a planar-lightwave-circuit-type asymmetric Mach-Zehnder interferometer on Si," in *IEEE Photonics Technology Letters*, vol. 8, no. 1, pp. 84-86,

[3] Lumerical MODE software. https://www.lumerical.com/

[4] Lumerical INTERCONNECT software. https://www.lumerical.com/

[5] KLayout software. https://www.klayout.de/

[6] L. Chrostowski and M. Hochberg, “Silicon Photonics Design: From Devices to Systems”, Cambridge University Press, 2015.

[7] Tiago Lima, “Design, Fabrication and Analysis of Interferometers in SOI photonics”